

See discussions, stats, and author profiles for this publication at: <https://www.researchgate.net/publication/281483499>

Substrate-Assisted and Enzymatic Pretransfer Editing of Nonstandard Amino Acids by Methionyl-tRNA Synthetase

ARTICLE in BIOCHEMISTRY · AUGUST 2015

Impact Factor: 3.02 · DOI: 10.1021/acs.biochem.5b00588 · Source: PubMed

READS

22

4 AUTHORS, INCLUDING:



Mohamed Aboelnga

University of Windsor

7 PUBLICATIONS 61 CITATIONS

SEE PROFILE



James Gauld

University of Windsor

80 PUBLICATIONS 1,260 CITATIONS

SEE PROFILE

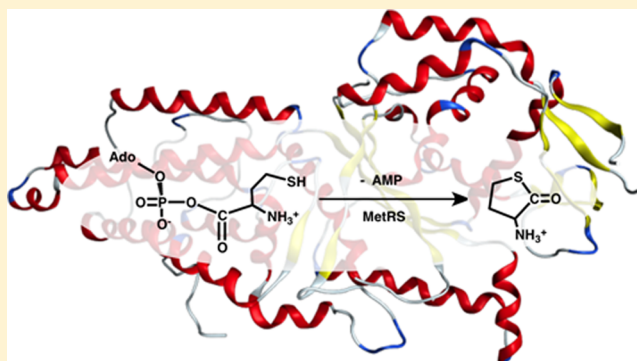
Substrate-Assisted and Enzymatic Pretransfer Editing of Nonstandard Amino Acids by Methionyl-tRNA Synthetase

Grant B. Fortowsky, Daniel J. Simard, Mohamed M. Aboelnga, and James W. Gauld*

Department of Chemistry and Biochemistry, University of Windsor, Windsor, Ontario N9B 3P4, Canada

S Supporting Information

ABSTRACT: Aminoacyl-tRNA synthetases (aaRSs) are central to a number of physiological processes, including protein biosynthesis. In particular, they activate and then transfer their corresponding amino acid to the cognate tRNA. This is achieved with a generally remarkably high fidelity by editing against incorrect standard and nonstandard amino acids. Using docking, molecular dynamics (MD), and hybrid quantum mechanical/molecular mechanics methods, we have investigated mechanisms by which methionyl-tRNA synthetase (MetRS) may edit against the highly toxic, noncognate, amino acids homocysteine (Hcy) and its oxygen analogue, homoserine (Hse). Substrate-assisted editing of Hcy-AMP in which its own phosphate acts as the mechanistic base occurs with a rate-limiting barrier of 98.2 kJ mol^{-1} . This step corresponds to nucleophilic attack of the Hcy side-chain sulfur at its own carbonyl carbon (C_{Carb}). In contrast, a new possible editing mechanism is identified in which an active site aspartate (Asp259) acts as the base. The rate-limiting step is now rotation about the substrate's aminoacyl $C\beta-C\gamma$ bond with a barrier of 27.5 kJ mol^{-1} , while for Hse-AMP, the rate-limiting step is cleavage of the $C_{\text{Carb}}-\text{OP}$ bond with a barrier of 30.9 kJ mol^{-1} . A similarly positioned aspartate or glutamate also occurs in the homologous enzymes LeuRS, IleRS, and ValRS, which also discriminate against Hcy. Docking and MD studies suggest that at least in the case of LeuRS and ValRS, a similar editing mechanism may be possible.



Enzymes catalyze many of the rich variety of chemical reactions essential for life and, furthermore, often do so with outstanding efficiencies. A key aspect of how they are able to perform such a role so effectively is their often high specificity, both in terms of substrate(s) on which the enzyme acts and the reaction(s) it can perform. As a result, there is considerable interest in understanding how they are able to achieve such remarkable specificity.^{1–3}

Aminoacyl-tRNA synthetases (aaRSs) make up a ubiquitous class of enzymes that has been attracting an increasing amount of attention. This is in part due to their central role in protein biosynthesis, as well as a diverse range of biochemical processes, including inflammation, cell death, and viral assembly.^{4–6} More specifically, they catalyze the activation of their corresponding amino acid and the subsequent aminoacylation of their cognate tRNA (tRNA^{aa}).^{7,8} These reactions are thought to proceed via substrate-assisted mechanisms in which the substrates themselves catalyze their transfer onto the tRNA^{aa} .^{9,10} Central to their physiological roles, however, is the difficult yet essential task of discriminating between amino acids. Indeed, it has been suggested that the error rate in translation cannot exceed 10^{-4} for proper growth and function.^{11,12} This can be particularly problematic for aaRSs whose cognate amino acid is structurally similar or isoelectronic with another. For example, ThrRS must discern its substrate threonine from serine and valine.^{9,13,14} This matter is further complicated as aaRSs must also discriminate against other species such as the nonstandard amino acids

homocysteine (Hcy) and homoserine (Hse).^{15–17} The latter are highly reactive, and their incorporation into proteins has been implicated in a number of diseases, including stroke, cancer, and Alzheimer's.¹⁸

Some aaRSs are able to achieve remarkably high fidelity within their aminoacylation active site. For example, cysteinyl-tRNA synthetase is able to discriminate its intended substrate cysteine from serine by a factor of 10^8 .¹⁹ However, many aminoacyl-tRNA synthetases have developed alternate approaches to help ensure a high level of accuracy.^{11,20} More specifically, they utilize pre- and/or post-transfer editing.²¹ In pretransfer editing, discrimination against non-native substrates generally occurs within the aminoacylation active site prior to aminoacylation of their cognate tRNA (tRNA^{aa}).^{22,23} In contrast, post-transfer editing typically utilizes a second active site, the editing site, whose role is to remove the aminoacyl moiety from misacylated tRNA.^{13,21,24} For example, threonyl-tRNA synthetase is thought to discern among threonine, serine, and valine^{9,13,14} via a double-sieve model.^{25,26} First, its aminoacylation site acts to exclude valine, while its editing site catalyzes the hydrolytic removal of serinyl from misacylated tRNA^{Thr} . ProRS is thought to edit against both alanine and cysteine by a triple-sieve mechanism.²⁷ A second

Received: June 1, 2015

Revised: August 25, 2015

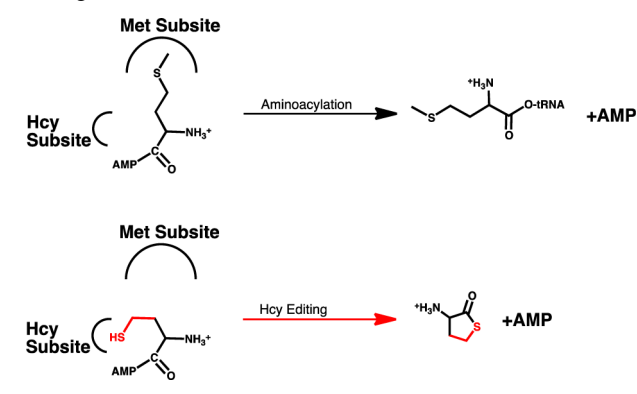
Published: August 31, 2015



editing site hydrolytically cleaves mischarged Ala-tRNA^{Pro},²⁸ while a YbaK protein is proposed to provide a third editing site^{29–31} to cleave mischarged cysteine-tRNA^{Pro} through a self-cyclization mechanism.^{27,32} It is noted that X-ray crystal structures of the editing domain of IleRS indicate that it can recognize both misactivated valine (Val-AMP) and its Val-misacylated cognate tRNA (Val-tRNA^{Ile}). Thus, pretransfer editing has been proposed to be possible also in the editing site.³³ However, whether this in fact occurs has been questioned because of a lack of evidence to support the corresponding return journey of the correct aminoacyl adenylate.²²

In particular, methionyl-tRNA synthetase (MetRS) has been suggested to be able to discriminate its native methionyl (Met) substrate from the nonstandard amino acid homocysteine (Hcy).^{16,17,34} In experimental rapid quenching studies of MetRS without its cognate tRNA present, a significant rate of hydrolysis of misactivated Hcys was observed.^{34,35} Thus, it was proposed that MetRS uses a pretransfer editing-type approach in which the active site pocket exploits differences in binding positions of the two aa-AMPs (Scheme 1).^{16,17,35,36} In the case of

Scheme 1. Illustration of the MetRS-Catalyzed (i) Aminoacyl Transfer Reaction for Met and (ii) Proposed^{16,17,34} Hcy-AMP Editing Mechanism



Met-AMP, a Met-binding subsite induces the methionyl moiety to bind in a linear-like fashion, suitably positioning it for aminoacyl transfer onto the cognate tRNA^{Met}.³⁷ In contrast, in the case of Hcy, a Hcy-binding subsite and the active site environment result in it preferentially binding in a bent or curled

position.³⁵ Significantly, as a result, its thiol tail is closer to its carbonyl carbon (C_{carb}) center. Indeed, the thiol sulfur is now well-positioned to nucleophilically attack C_{carb}, leading to cleavage of the Met–O_{AMP} bond and formation of a cyclic thiolactone. That is, editing via a self-cyclization mechanism is enhanced.

However, this proposal is not without some controversy. In particular, site-directed mutagenesis studies were unable to definitively confirm or refute the proposed thiol-binding subsite.³⁸ Furthermore, it has been noted that Hcy is arguably the most reactive amino acid.^{18,39} Hence, by the simple release of Hcy-AMP from the active site of MetRS, self-cyclization may occur.³⁸

In the study presented here, a multiscale computational approach has been used to investigate possible pretransfer editing mechanisms by which methionyl-tRNA synthetase (MetRS) may discriminate against the toxic nonstandard amino acids homocysteine (Hcy) and homoserine (Hse). In particular, docking, molecular dynamics (MD), and quantum mechanical/molecular mechanics (QM/MM) methods have been applied. In addition, the applicability of such editing mechanisms to several other aminoacyl-tRNA synthetases that also edit against Hcy and Hse has also been considered.

COMPUTATIONAL METHODS

MD Simulations. Molecular Operating Environment (MOE) was used for model preparation and determination of the binding orientation of the substrate within the active site.⁴⁰ Appropriate X-ray crystal structures of the aaRSs considered herein [Protein Data Bank (PDB) entries 2CT8 (MetRS),⁴¹ 1GAX (ValRS),⁴² 1JZQ (IleRS),⁴² and 3ZGZ (LeuRS)⁴³] were used as templates with their bound substrates and/or substrate analogues being modified to Hcy-AMP or Hse-AMP, and missing hydrogen atoms were then added. The protonate three-dimensional application in MOE was used to assign each residue its ionization state. Each complex was then spherically solvated by adding a layer of water (740 molecules) to represent the solvent environment. The geometry of each complex was then optimized using the AMBER99 molecular mechanics force field until the root-mean-square deviation (rmsd) gradient of the energy fell below 0.01 kJ mol^{−1} Å^{−1}. This structure was used as the initial starting point for MD simulations in which all atoms were free to move. The MD simulations were performed using

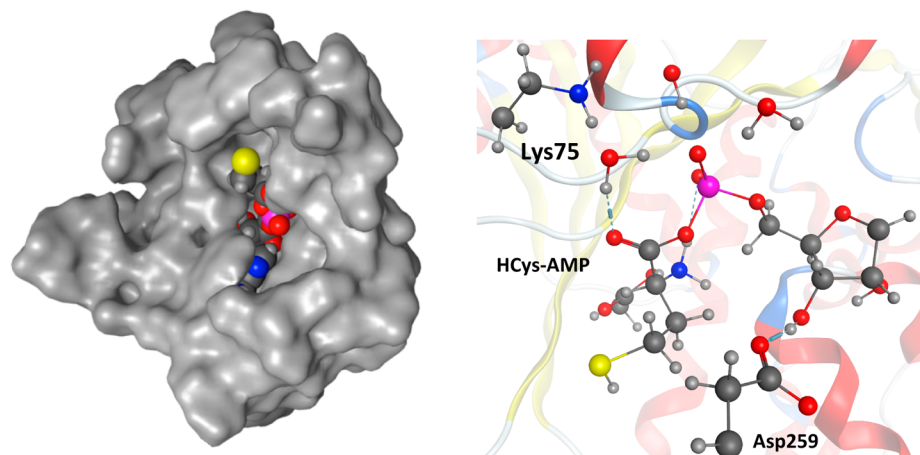


Figure 1. Schematic illustration of the QM/MM chemical model used for MetRS with Hcy-AMP bound within its active site. Atoms in the high (QM) layer are shown as balls and sticks, while for the sake of clarity, the MM layer has been omitted.

the NAMD program⁴³ under constant pressure and temperature, with a time step of 2 fs. Coulombic interactions were calculated using the PME method, while short-range van der Waals interactions were truncated at 8–10 Å. The system was initially equilibrated for 0.1 ns at 300 K followed by a production run within the *NPT* ensemble at 300 K and 1 bar for 10 ns. Structures were then clustered into 10 groups on the basis of active site rmsd, and the most representative average structure of the highest populated cluster was chosen as a starting point for the subsequent QM/MM model (see below).

ONIOM (QM/MM). All QM/MM calculations were performed within the ONIOM formalism as implemented in Gaussian 09.^{44–47} A suitable chemical model was derived from the chosen average structure described above by truncating the complex. Specifically, each model consisted of the substrate (e.g., Hcy-AMP) and extended outward to include the three surrounding layers of amino acids and consisted of more than 2000 atoms.

For the MetRS⋯substrate complex, the QM region consisted of the substrate (Hcy-AMP or Hse-AMP), Asp259 and backbone amide bonds, the R groups of active site residues Asp52 and Lys57, and three active site water molecules (Figure 1). Cartesian coordinates of the QM layer are provided in the Supporting Information (Table S1). All other residues and atoms were placed in the MM layer. All atoms in the QM region as well as all those within 10 Å of the substrate were free to move, while all others were held fixed at their MD-optimized positions. It should be noted that several models with systematically larger QM regions were initially used. The model described above is the one that was ultimately used for all mechanisms examined to facilitate their direct comparison. Optimized structures, frequencies, and Gibbs free energy corrections (ΔE_{Gibbs}) were obtained at the ONIOM [B3LYP/6-31G(d,p):AMBER96] level of theory within the mechanical embedding (ME) formalism.^{48–50} Some transition structures, ^{Hcy}TS1, ^{Hse}TS1, and ^{Hcy}TS2', were obtained by performing detailed potential energy surface scans. Relative free energies were obtained by performing single-point energy calculations at the ONIOM [B3LYP/6-311G(2df,p):Amber96] ME level of theory on the optimized structures described above, with inclusion of the appropriate ΔE_{Gibbs} correction.

RESULTS AND DISCUSSION

Substrate Binding. As noted above, it has been suggested that within the active site of MetRS the native substrate methionine (Met) may bind in a linear fashion while the noncognate substrate homocysteine (Hcy) instead binds in a nonlinear, or bent, position.^{37,51} Hence, the binding of the native substrate Met-AMP as well as the possible alternate substrates Hcy-AMP and Hse-AMP, within the MetRS active site, was examined. Average structures of each of the three bound substrates mentioned above were obtained after 10 ns MD simulations (see Computational Methods) and are overlaid in Figure 2. Remarkably, as can be seen, they all preferentially bind in essentially the same linear position within the active site. Indeed, each remains quite similarly oriented, with the largest differences observed being in the positioning of the ends of their aminoacyl R groups, e.g., -SH, -OH, and -SCH₃. While the hydroxyl and thiol of Hse- and Hcy-AMP, respectively, are quite similarly positioned, the -SCH₃ group of Met-AMP is tilted down, though only slightly.

Substrate-Assisted Editing of Hcy. Possible mechanisms by which Hcy-AMP may cyclize within the active site of MetRS were then examined. For the reaction to occur, a base must

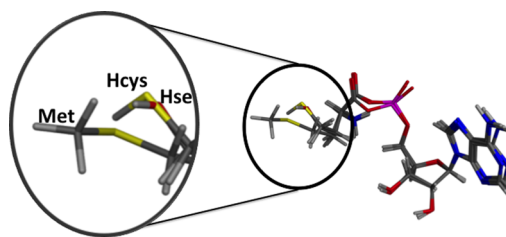


Figure 2. Overlaid average structures (see Computational Methods) of Met-, Hcy-, and Hse-AMP bound within the MetRS active site.

facilitate deprotonation of the thiol of the Hcy moiety for its sulfur to nucleophilically attack Hcy's own sp^2 carbonyl carbon (C_{carb}). Analogous to that generally proposed to occur in the substrate-assisted aminoacyl transfer reaction catalyzed by aaRSs, the ability of the Hcy-AMP's own phosphate group to act as the required base was examined.^{21,52} However, in the optimized structure of the bound MetRS⋯Hcy-AMP reactive complex (^{Hcy}RC), the distance between Hcy-AMP's sulfur (S_{Hcy}) and nearest phosphate oxygen (O_{phos}) is 7.15 Å while the other key distance, $\text{S}_{\text{Hcy}}\cdots\text{C}_{\text{carb}}$, is 3.94 Å (Figure 3). It is noted that over the course of the 10 ns MD simulation the average $\text{S}_{\text{Hcy}}\cdots\text{O}_{\text{phos}}$ distance was consistently near 7 Å (Figure S1). Hence, the substrate, or at least its thiol tail, must undergo a conformational change to better position the thiol for intramolecular attack at C_{carb} .

This conformational change can be achieved by rotation about the $\text{C}_{\beta}\text{--C}_{\gamma}$ bond of the R group of the Hcy moiety via ^{Hcy}TS1 with a barrier of 27.5 kJ mol^{−1} to give the alternate substrate-bound MetRS⋯Hcy-AMP complex ^{Hcy}I1 lying marginally lower in energy than ^{Hcy}RC by 1.0 kJ mol^{−1} (Figure 4). The Hcy has consequently changed conformation from being essentially linear to bent. In ^{Hcy}I1, the substrate's thiol moiety now forms a moderately strong hydrogen bond with the R group carboxylate oxygen of Asp259, as indicated by an $\text{Asp259COO}^-\cdots\text{HS}_{\text{Hcy}}$ distance of 1.95 Å (Figure 3). Importantly, with respect to a substrate-assisted mechanism, the $\text{S}_{\text{Hcy}}\cdots\text{C}_{\text{carb}}$ distance has decreased by 0.65 Å to 3.29 Å while the $\text{S}_{\text{Hcy}}\cdots\text{O}_{\text{phos}}$ distance has decreased significantly by 1.53 Å to 5.62 Å but clearly is still quite sizable (Figure 3).

The next and final step in the mechanism is nucleophilic attack of Hcy's sulfur at its own C_{carb} center with concomitant intramolecular transfer of its thiol proton onto its nearest nonbridging phosphate oxygen. This occurs via cyclic transition state ^{Hcy}TS2 with a significantly larger barrier of 98.2 kJ mol^{−1} and as a result is the rate-limiting step of the reaction (Figure 4). In ^{Hcy}TS2, the thiol's $\text{S}_{\text{Hcy}}\text{--H}$ bond has lengthened significantly to 1.78 Å, while the $\text{S}_{\text{Hcy}}\text{H}\cdots\text{O}_{\text{phos}}$ distance has decreased markedly to 1.12 Å. Concomitantly, the $\text{S}_{\text{Hcy}}\cdots\text{C}_{\text{carb}}$ distance has decreased to 2.60 Å (Figure 3). Thus, it appears that proton transfer precedes formation of the $\text{C}_{\text{carb}}\text{--S}_{\text{Hcy}}$ bond and, hence, cleavage of the $\text{C}_{\text{carb}}\text{--OP}$ bond.

This step results in formation of the final product complex (^{Hcy}PC) lying 70.4 kJ mol^{−1} lower in energy than ^{Hcy}RC, indicating that the overall reaction is exergonic. In ^{Hcy}PC, a $\text{C}_{\text{carb}}\text{--S}_{\text{Hcy}}$ bond has been formed [$r(\text{C}_{\text{carb}}\text{--S}_{\text{Hcy}}) = 1.82$ Å] and the $\text{C}_{\text{carb}}\text{--OP}$ bond cleaved [$r(\text{C}_{\text{carb}}\cdots\text{OP}) = 3.34$ Å], giving the cyclic thiolactone derivative of Hcy and AMP bound within the MetRS active site.

It is noted that for Hcy-AMP with a neutral thiol the analogous self-cyclization mechanism in the gas phase is calculated to occur in one step with a modest reaction barrier of 52.7 kJ mol^{−1}.

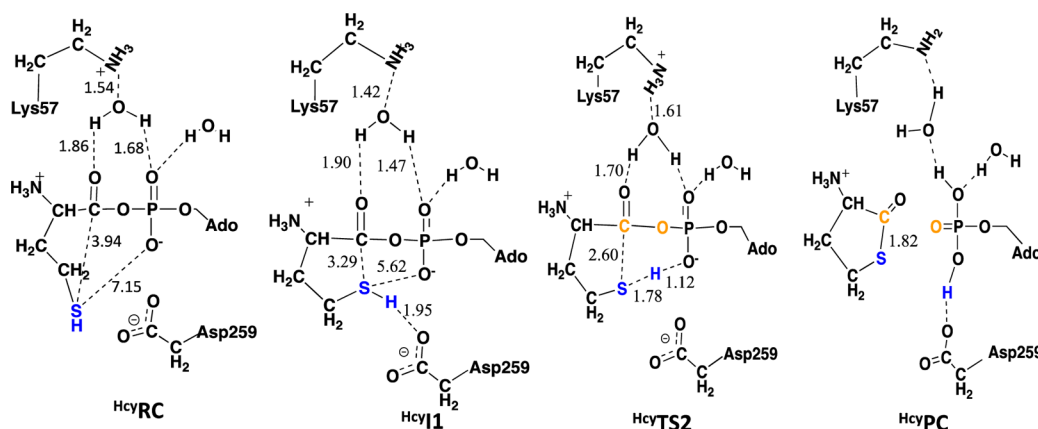


Figure 3. Schematic illustration of the optimized structures of the reactant and product complexes, intermediates, and transition structures obtained for the Hcy editing mechanism using the phosphate as the base, with selected bond lengths shown (angstroms).

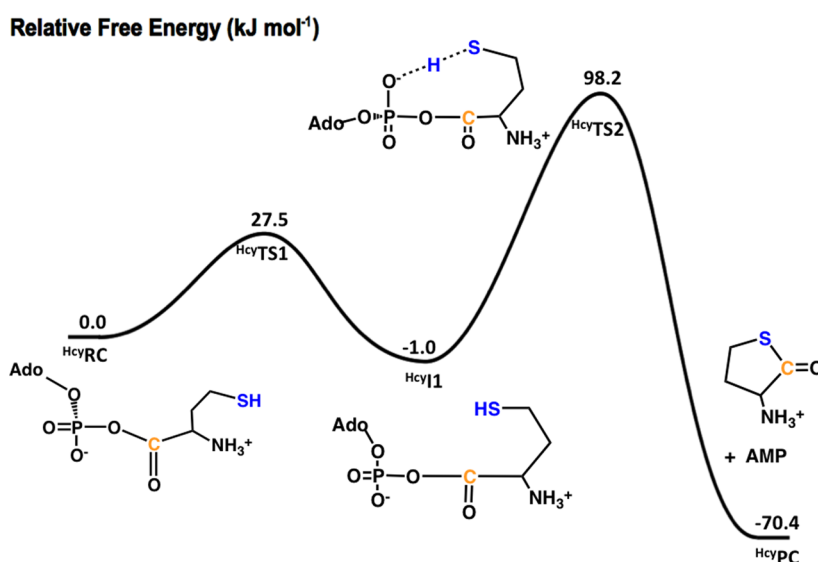


Figure 4. Relative free energy surface obtained (see Computational Methods) for substrate-assisted editing of Hcy-AMP by MetRS in which a nonbridging phosphate oxygen of Hcy-AMP acts as the mechanistic base.

Residue-Based Editing of Hcy. Unfortunately, no other functional groups within the substrate, e.g., the aminoacyl's amino group as recently suggested in the case of ThrRS,⁹ seem to be suitably positioned to potentially act as the required mechanistic base. However, as noted above, in the MetRS...Hcy-AMP complex ^{Hcy}I1, the thiol of the Hcy moiety is hydrogen bonded to the R group carboxylate of Asp259, suggesting that it may be a candidate for an alternate mechanistic base. Furthermore, the R group of Asp259 is surrounded by the hydrophobic residues Ile260, Trp288, and Val256 that will likely help elevate its pK_a . Indeed, using MOE,^{40,53} Asp259 is predicted to have an elevated pK_a value of 4.9 compared to most other Asp residues in MetRS that generally lie in the range of 2.3–4.0.

Indeed, in the MD simulations of the initial MetRS...Hcy-AMP complex, the average $Asp259COO^- \cdots S_{Hcy}$ distance is 5.30 Å (Figure S2). This is markedly shorter than the length of 7.15 Å observed for the $S_{Hcy} \cdots O_{phos}$ distance in the same complex. It is noted that the average $Asp259COO^- \cdots C_{carb}$ distance is 4.25 Å (Figure S3). In the QM/MM-optimized structure of the initial reactant complex (^{Hcy}RC), the Asp259 carboxylate is calculated to lie almost equidistant from S_{Hcy} and C_{carb} with $Asp259COO^- \cdots S_{Hcy}$ and $Asp259COO^- \cdots C_{carb}$ distances of 5.20 and 5.03 Å,

respectively (Figure 5). In the intermediate complex ^{Hcy}I1 in which the tail has undergone a conformational change, these distances are shortened to 3.31 and 4.95 Å, respectively (Table S1). Consequently, we examined possible mechanisms by which the active site residue Asp259 may directly help catalyze the editing of Hcy by MetRS.

When Hcy-AMP is bound within the active site of MetRS, the carbonyl oxygen (O_{carb}) of its Hcy moiety and a nonbridging oxygen of its phosphate hydrogen bond to the same active site-bound water molecule. Importantly, this water is simultaneously hydrogen bonded to the protonated side-chain amino group of Lys57. This network of hydrogen bonds is maintained in ^{Hcy}I1, and upon its formation, the $Lys57NH_3^+$ group is able to essentially transfer a proton via the water onto a nonbridging phosphate oxygen of Hcy-AMP. This is calculated to occur via ^{Hcy}TS3' effectively without a barrier at 298 K, as indicated by the marginally lower relative free energy of ^{Hcy}TS3' compared to that of ^{Hcy}I1 (Figure 6).

This transfer results in formation of the alternate MetRS...Hcy-AMP complex ^{Hcy}I2' lying 44.9 kJ mol⁻¹ lower in energy than ^{Hcy}RC (Figure 6). The largest structural changes observed upon going from ^{Hcy}I1 to ^{Hcy}I2' are seen in the P–O bond for the

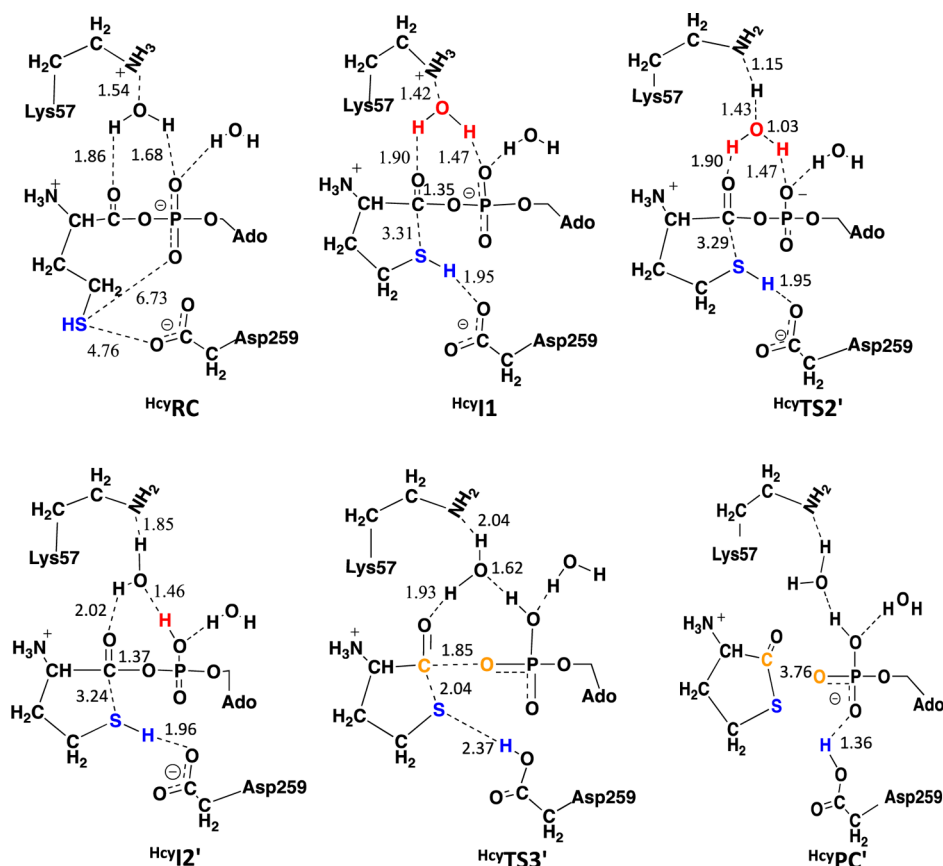


Figure 5. Schematic illustration of the optimized structures of the reactant and product complexes, intermediates, and transition structures obtained for the Hcy editing mechanisms, with selected bond lengths shown (angstroms).

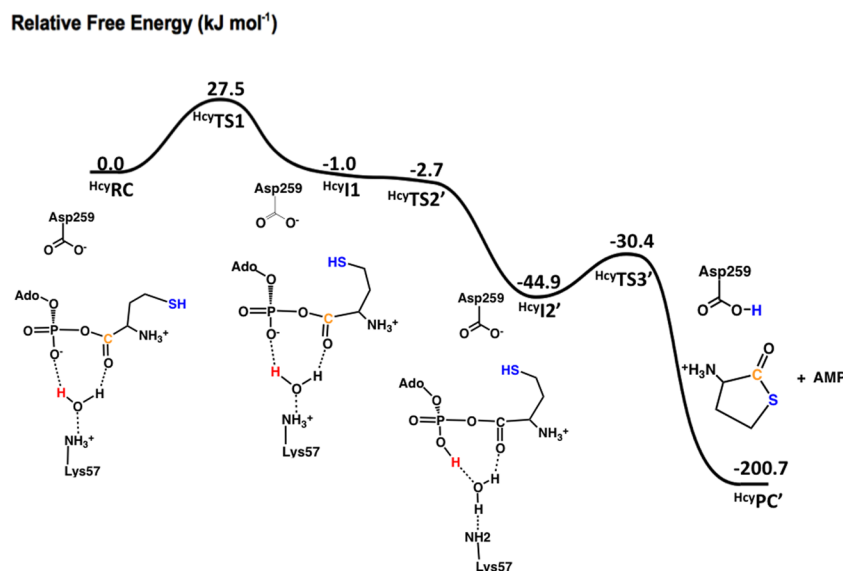


Figure 6. Relative free energy surface obtained (see Computational Methods) for editing of Hcy-AMP by MetRS in which Asp259 acts as the mechanistic base.

nonbridging oxygen that is protonated, which lengthens from 1.53 to 1.57 Å. Additionally, the C_{carb}–OP bond is elongated from 1.35 to 1.37 Å, while the S_{Hcy}...C_{carb} distance decreases from 3.31 to 3.24 Å. It is noted that only quite minor changes are observed in the S_{Hcy}...OOC_{Asp259} hydrogen bond interaction.

The next and final step is nucleophilic attack of the thiol S_{Hcy} sulfur at C_{carb} with concomitant transfer of the thiol proton onto

the side-chain carboxyl of Asp259. This reaction proceeds via HcyTS3' with a barrier of just 14.5 kJ mol⁻¹ relative to HcyI2' to give the final product complex (HcyPC'), the Hcy-derived cyclic thiolactone and AMP bound in the active site of MetRS. As for the substrate-assisted mechanism, the final product complex is calculated to lie markedly lower in energy than HcyRC; i.e., the mechanism is exergonic. Importantly, this barrier via HcyTS3' is

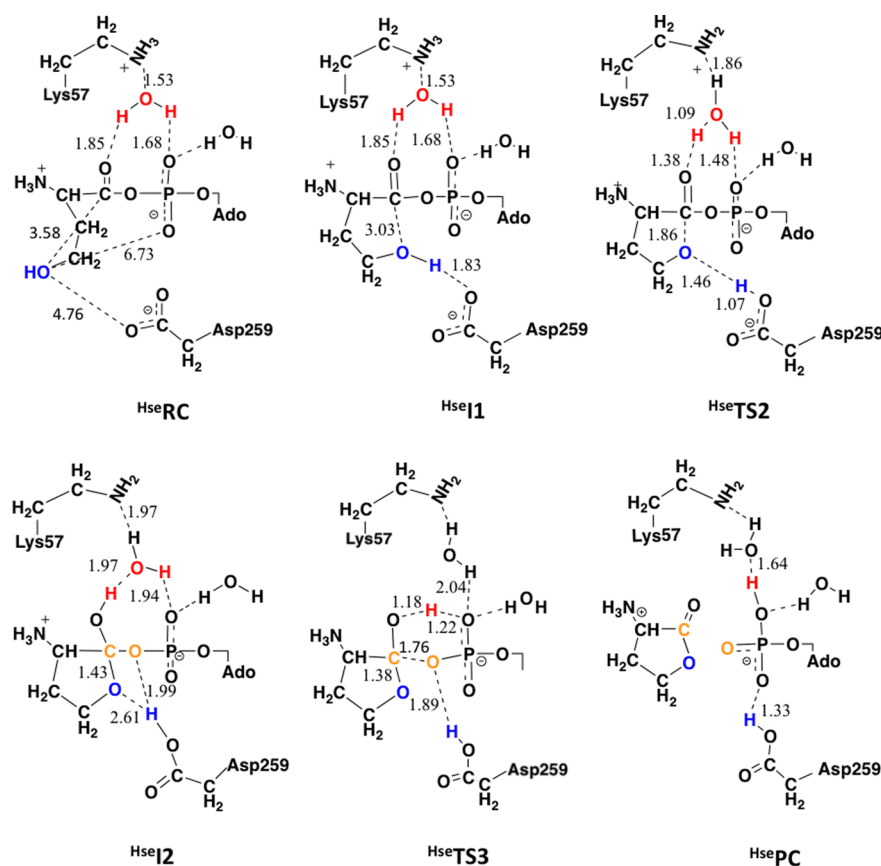


Figure 7. Schematic illustration of the optimized structures of the reactant and product complexes, intermediates, and transition structures obtained for the Hse editing mechanism in which Asp259 acts as the base, with selected bond lengths shown (angstroms).

84.5 kJ mol⁻¹ lower in energy than the analogous second step in the substrate-assisted mechanism described above in which the Hcy-AMP's own phosphate acts as the base (Figure 4). As a result, the overall rate-limiting step is now the initial conformational change in the substrate's Hcy side chain with a barrier of just 27.5 kJ mol⁻¹ (Figure 6).

The effects of mutating Asp259 to alanine were also considered (Table S1). Notably, it was found that in the mutated enzyme the corresponding first intermediate complex is now destabilized relative to the Asp259Ala-mutated reactive complex, lying 11 kJ mol⁻¹ higher in energy. However, the Hcy-AMP thiol may naturally occur to some extent in its deprotonated state. Hence, the possible structure of the Asp259Ala mutated enzyme–deprotonated Hcy-AMP complex was examined. In this latter case, a TS for bending of the tail could not be optimized as even slight bending led to an intermediate complex in which the S...C_{carb} bond has started to form [$r(\text{S}\cdots\text{C}_{\text{carb}}) = 1.93 \text{ \AA}$] while the C_{carb}–O_{phos} bond has lengthened by 0.05 Å. It is noted that a similar result was obtained for the native enzyme (not shown). This suggests that in an Asp259Ala mutated MetRS substrate-assisted editing may still be feasible.

Residue-Based Editing of Hse. However, it has been previously suggested that Hcy is arguably one of the most reactive amino acids that could be incorporated into a protein.³⁴ This is due in part to the pK_a of its thiol, and thus, it is probable that Hcy-AMP may also nonenzymatically self-cyclize in solution. Its oxygen analogue homoserine (Hse), however, is less reactive, and its R group hydroxyl has a higher pK_a. Given that sulfur and oxygen are isoelectronic and that LysRS has been proposed to be able to edit both Hse-AMP and Hcy-AMP,⁵⁴ a

similar possibility was considered for MetRS. Thus, we also examined the ability of Asp259 to act as a suitable mechanistic base to allow MetRS to edit against Hse.

The results of the molecular dynamics simulations revealed large similarities in the positions of the MetRS active site residues when either Hcy-AMP or Hse-AMP is bound, as indicated by comparative rmsd of just 0.41 Å. In the case of Hse-AMP, the average distance between the side-chain hydroxyl oxygen (O_s) of Hse and the nearest AMP phosphate oxygen is slightly shorter than that observed in the MetRS...Hcy-AMP complex at 6.65 Å (Figure S4). Meanwhile, the average distance between O_s and the nearest initial Asp259 side-chain carboxylate oxygen is 5.21 Å (Figure S5A). However, it should be noted that unlike in the case of the MetRS...Hcy-AMP complex, the Asp259 carboxylate rotated during the 10 ns simulation. When we consider the average O_s...OAsp259 distance taking both Asp259 carboxylate oxygens into account, it is considerably shorter (4.28 Å). Furthermore, the average distance between O_s and the carboxylate carbon of Asp259 is consistently near 5.71 Å (Figure S5B).

The QM/MM-optimized structure of the initial MetRS...Hse-AMP complex (^{Hse}RC) is given in Figure 7. Similar to that observed in the analogous Hcy complex ^{Hcy}RC, the distance between O_s and the nearest phosphate oxygen (6.73 Å) is significantly greater than that between O_s and the nearest Asp259 carboxylate oxygen (4.76 Å). As observed for Hcy-AMP, the MetRS-bound Hse-AMP is able to undergo a conformational change via rotation about the C_β–C_γ bond of the R group of the Hse. This reaction proceeds via ^{Hse}TS1 with a barrier slightly lower than that observed for MetRS-bound Hcy-AMP of just

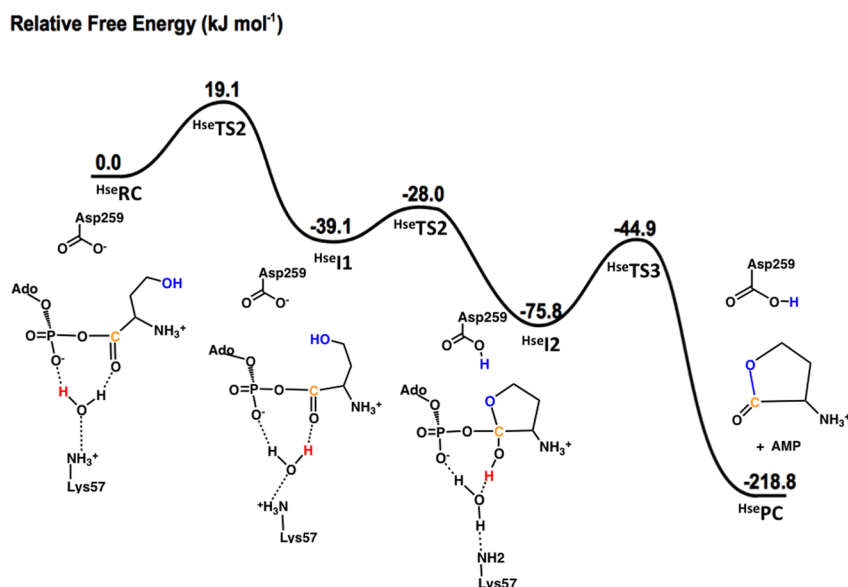


Figure 8. Relative free energy surface obtained (see [Computational Methods](#)) for editing of Hse-AMP by MetRS in which Asp259 acts as the mechanistic base.

19.1 kJ mol⁻¹ (Figure 8). The resulting alternate substrate-bound MetRS⋯Hse-AMP complex (^{Hse}I1), however, lies noticeably lower in energy than ^{Hse}RC by 39.1 kJ mol⁻¹.

In ^{Hse}I1, the side-chain hydroxyl of Hse-AMP forms a short strong hydrogen bond to the carboxylate of Asp259 [*r*(-O_SH⋯OOC_{Asp259}) = 1.83 Å]. The O_S center is now nicely positioned just 3.03 Å from the C_{carb} center. It is noted that the Asp259COO⁻⋯C_{carb} distance has decreased from 5.00 to 4.73 Å.

The next step involves proton transfer from the side-chain protonated amino group of Lys57 onto the carbonyl oxygen of the Hse moiety of the substrate. Furthermore, this occurs with concomitant transfer of the Hse moieties; the O_SH proton is transferred onto the carboxylate of Asp259, and concomitantly, the O_S center nucleophilically attacks C_{carb} to form a cyclic tetrahedral intermediate. This process occurs via ^{Hse}TS2 at a cost of just 11.1 kJ mol⁻¹, with the resulting cyclic intermediate ^{Hse}I2 lying much lower in energy than ^{Hse}RC by 75.8 kJ mol⁻¹ (Figure 8). In ^{Hse}I2, the newly formed single C_{carb}–O_S bond has a length of 1.43 Å, while the C_{carb}–OP bond has lengthened markedly by 0.09 Å to 1.44 Å. In addition, the now neutral carboxylate of Asp259 forms a hydrogen bond with the C_{carb}–OP oxygen as indicated by an Asp259COOH⋯OP distance of 1.99 Å. This would help to stabilize the buildup of negative charge on the bridging oxygen as the C_{carb}–OP bond is cleaved.

The next and final step is cleavage of the PO–C_{carb} bond to give AMP and a cyclic lactone Hse derivative. This occurs with concomitant proton transfer effectively from the C_{carb}–OH hydroxyl via the bridging water newly formed alcohol to the phosphate of the cleaving AMP moiety. Notably, this reaction step has a barrier slightly higher than that obtained for Hcy-AMP of 30.9 kJ mol⁻¹ and in fact is the rate-limiting step in editing of Hse-AMP by MetRS. This editing reaction is similar to the second-half reaction of aaRSs, aminoacylation of their cognate tRNA via deprotonation of an alcohol with concomitant nucleophilic attack at an sp² carbon.

Editing of Hcy and Hse in Related aaRSs. The results described above suggest that for both Hcy-AMP and Hse-AMP the active site residue Asp259 could effectively act as a mechanistic base in editing by MetRS. However, it has been

noted that some other aaRSs such as the structurally homologous ValRS, IleRS, and LeuRS may bind these nonstandard amino acids and potentially also edit against Hcy and Hse.¹⁵ Thus, we considered the binding modes of Hcy and Hse within the active sites of these other aaRSs and whether they may also contain similarly basic and positioned residues. As observed with MetRS, Hcy- and Hse-AMP bind in similar positions to each other within the active site of each of ValRS, LeuRS, and IleRS. Thus, for the sake of simplicity, only the results obtained for Hcy-AMP are discussed herein unless otherwise noted.

Remarkably, ValRS, LeuRS, and IleRS are observed to have an active site aspartyl (Asp490) or glutamyl (Glu532 or Glu550) residue in the same approximate position relative to the substrate's C_{carb} center as the aspartyl (Asp259) in MetRS. Furthermore, the Hcy-AMP substrate binds within their active sites in a linear-like conformation similar to that observed in MetRS. Consequently, the positions of the carboxylate groups of Asp490, Glu532, and Glu550 with respect to the bound Hcy-AMP substrate are in reasonable agreement with that observed in MetRS. For example, the average C_{carb}⋯O_{Asp/Glu} distances all lie within 1.16 Å of each other, ranging from 4.10 Å (IleRS) to 5.26 Å (ValRS) (Table 1). Furthermore, all S_{Hcy}⋯C_{carb} distances are within 1.24 Å of each other, from 3.91 Å in MetRS to 5.19 Å in LeuRS (Table 1). More importantly, as in the case of MetRS, for both LeuRS and ValRS, the average S_{Hcy}⋯O_{Asp/Glu} distance is significantly shorter than the average S_{Hcy}⋯O_{phos} distance by 2.27 and 2.06 Å, respectively. The exception is IleRS in which the average S_{Hcy}⋯O_{phos} distance is shorter than the S_{Hcy}⋯O_{Asp/Glu}

Table 1. Selected Average Distances (angstroms) Obtained from 10 ns MD Simulations When Hcy-AMP Bound in the Active Site of MetRS, LeuRS, ValRS, and IleRS

	average distance (Å)			
	MetRS	LeuRS	ValRS	IleRS
S _{Hcy} ⋯O _{phos}	6.99	7.78	7.01	4.25
S _{Hcy} ⋯O _{Asp/Glu}	5.30	5.51	4.94	4.70
S _{Hcy} ⋯C _{carb}	3.91	5.19	4.14	4.66
O _{Asp/Glu} ⋯C _{carb}	4.25	4.39	5.26	4.10

distance by 0.45 Å; thus, it is less clear which editing mechanism if any may be available to the enzyme.

CONCLUSION

We have used a complementary computational approach, combining molecular dynamics (MD) and hybrid quantum mechanical/molecular mechanics (QM/MM) methods, to investigate the mechanism by which methionyl-tRNA synthetase (MetRS) may edit against the noncognate and highly toxic amino acid homocysteine (Hcy) and its oxygen analogue, homoserine (Hse). In addition, we have also examined the binding of Hcy and Hse within the related enzymes LeuRS, ValRS, and IleRS.

These results suggest that the phosphate group of Hcy, analogous to the generally held substrate-assisted aminoacyl transfer mechanism of aaRSs, could potentially act as a base to facilitate editing of Hcy and Hse. The rate-limiting step is nucleophilic attack of the side-chain thiol sulfur (S_{Hcy}) at the substrate's own carbonyl carbon (C_{carb}) center with a barrier of 98.2 kJ mol⁻¹.

However, a considerably energetically more favorable editing mechanism was obtained in which the MetRS active site residue Asp259 plays an essential role as a mechanistic base. That is, MetRS can exploit enzymatic editing for such amino acids. The rate-limiting step for Hcy-AMP cleavage via intramolecular cyclization in MetRS is the initial required rotation about the substrate's aminoacyl C_{β} – C_{γ} bond with a barrier of just 27.5 kJ mol⁻¹. For editing of Hse-AMP, the rate-limiting step is cleavage of the PO– C_{carb} bond with a barrier of only 30.9 kJ mol⁻¹.

In addition, ValRS, LeuRS, and IleRS, which likely also edit against Hcy and Hse, have active site motifs similar to that of MetRS. In particular, all contain a similarly positioned residue carboxylate, be it either an Asp (MetRS and ValRS) or a Glu (LeuRS and IleRS). Furthermore, Hcy-AMP and Hse-AMP preferentially bind in similar “linear” positions in all four aaRSs: MetRS, LeuRS, IleRS, and ValRS. These enzyme–substrate structures suggest that at least in the case of LeuRS and ValRS, a similar editing mechanism may be possible.

ASSOCIATED CONTENT

Supporting Information

The Supporting Information is available free of charge on the ACS Publications website at DOI: 10.1021/acs.biochem.5b00588.

Cartesian coordinates and energies of the optimized structures reported here (PDF)

AUTHOR INFORMATION

Corresponding Author

*E-mail: gauld@uwindsor.ca. Telephone: +1-519-253-3000, ext. 3992. Fax: +1-519-973-7098.

Funding

This work was supported by grants from the Natural Sciences and Engineering Research Council of Canada (NSERC). D.J.S. also thanks the NSERC CGS-Master's program for financial support.

Notes

The authors declare no competing financial interest.

ACKNOWLEDGMENTS

We thank Compute Canada and SHARCNET for additional computational resources.

ABBREVIATIONS

aaRS, aminoacyl-tRNA synthetases; MetRS, methionyl-tRNA synthetase; Hcy, homocysteine; Hse, homoserine; AMP, adenosine monophosphate; C_{carb} , carbonyl carbon; QM/MM, quantum mechanical/molecular mechanics; MD, molecular dynamics; MOE, Molecular Operating Environment; ME, mechanical embedding.

REFERENCES

- (1) Ramos, M. J., and Fernandes, P. A. (2008) Computational Enzymatic Catalysis. *Acc. Chem. Res.* 41, 689–698.
- (2) Jencks, W. P. (1987) *Catalysis in Chemistry and Enzymology*, John Wiley & Sons, Inc., New York.
- (3) Jorge, L., and Gaudl, J. W. (2010) Mechanistics of Enzyme Catalysis: From Small to Large Active-Site Models. In *Quantum Biochemistry* (Matta, C. F., Ed.) pp 643–666, Wiley-VCH Verlag GmbH & Co. KGaA, Berlin.
- (4) Hausmann, C. D., and Ibba, M. (2008) Aminoacyl-tRNA synthetase complexes: molecular multitasking revealed. *Fems Microbiol. Rev.* 32, 705–721.
- (5) Dewan, V., Liu, T., Chen, K. M., Qian, Z. Q., Xiao, Y., Kleiman, L., Mahasen, K. V., Li, C. L., Matsuo, H., Pei, D. H., and Musier-Forsyth, K. (2012) Cyclic Peptide Inhibitors of HIV-1 Capsid-Human Lysyl-tRNA Synthetase Interaction. *ACS Chem. Biol.* 7, 761–769.
- (6) Wang, J., Fang, P. F., Schimmel, P., and Guo, M. (2012) Side Chain Independent Recognition of Aminoacyl Adenylates by the Hint1 Transcription Suppressor. *J. Phys. Chem. B* 116, 6798–6805.
- (7) Cusack, S. (1997) Aminoacyl-tRNA synthetases. *Curr. Opin. Struct. Biol.* 7, 881–889.
- (8) Safo, M. G., and Moor, N. A. (2009) Codases: 50 years after, J. *Mol. Biol.* 43, 211–222.
- (9) Huang, W. J., Bushnell, E. A. C., Francklyn, C. S., and Gaudl, J. W. (2011) The alpha-Amino Group of the Threonine Substrate as The General Base During tRNA Aminoacylation: A New Version of Substrate-Assisted Catalysis Predicted by Hybrid DFT. *J. Phys. Chem. A* 115, 13050–13060.
- (10) Liu, H. N., and Gaudl, J. W. (2008) Substrate-assisted Catalysis in the Aminoacyl Transfer Mechanism of Histidyl-tRNA Synthetase: A Density Functional Theory Study. *J. Phys. Chem. B* 112, 16874–16882.
- (11) Ibba, M., and Soll, D. (1999) Quality control mechanisms during translation. *Science* 286, 1893–1897.
- (12) Reynolds, N. M., Lazazzera, B. A., and Ibba, M. (2010) Cellular mechanisms that control mistranslation. *Nat. Rev. Microbiol.* 8, 849–856.
- (13) Minajigi, A., and Francklyn, C. S. (2010) Aminoacyl Transfer Rate Dictates Choice of Editing Pathway in Threonyl-tRNA Synthetase. *J. Biol. Chem.* 285, 23810–23817.
- (14) Sankaranarayanan, R., Dock-Bregeon, A. C., Rees, B., Bovee, M., Caillet, J., Romby, P., Francklyn, C. S., and Moras, D. (2000) Zinc ion mediated amino acid discrimination by threonyl-tRNA synthetase. *Nat. Struct. Biol.* 7, 461–465.
- (15) Jakubowski, H. (2001) Translational accuracy of aminoacyl-tRNA synthetases: Implications for atherosclerosis. *J. Nutr.* 131, 2983S–2987S.
- (16) Jakubowski, H. (2011) Quality control in tRNA charging - editing of homocysteine. *Acta Biochim. Polym.* 58, 149–163.
- (17) Jakubowski, H. (2012) Quality control in tRNA charging. *Wiley Interdiscip. Rev. RNA* 3, 295–310.
- (18) Jakubowski, H. (2004) Molecular basis of homocysteine toxicity in humans. *Cell. Mol. Life Sci.* 61, 470–487.
- (19) Zhang, C., Christian, T., Newberry, K., Perona, J., and Hou, Y. (2003) Zinc-mediated amino acid discrimination in cysteinyl-tRNA synthetase. *J. Mol. Biol.* 327, 911–917.
- (20) Perona, J. J., Rould, M. A., and Steitz, T. A. (1993) Structural basis for transfer RNA aminoacylation by Escherichia coli glutamyl-tRNA synthetase. *Biochemistry* 32, 8758–8771.
- (21) Perona, J., and Gruic-Sovulj, I. (2013) *Synthetic and Editing Mechanisms of Aminoacyl-tRNA Synthetases*, pp 1–41, Springer, Berlin.

- (22) Gruic-Sovulj, I., Rokov-Plavec, J., and Weygand-Durasevic, I. (2007) Hydrolysis of non-cognate amino acyl-adenylates by a class II aminoacyl-tRNA synthetase lacking an editing domain. *FEBS Lett.* 581, 5110–5114.
- (23) Dulic, M., Perona, J. J., and Gruic-Sovulj, I. (2014) Determinants for tRNA-Dependent Pretransfer Editing in the Synthetic Site of Isoleucyl-tRNA Synthetase. *Biochemistry* 53, 6189–6198.
- (24) Fukunaga, R., Fukai, S., Ishitani, R., Nureki, O., and Yokoyama, S. (2004) Crystal structures of the CP1 domain from *Thermus thermophilus* isoleucyl-tRNA synthetase and its complex with L-valine. *J. Biol. Chem.* 279, 8396–8402.
- (25) Beebe, K., Merriman, E., de Pouplana, L. R., and Schimmel, P. (2004) A domain for editing by an archaeobacterial tRNA synthetase. *Proc. Natl. Acad. Sci. U. S. A.* 101, 5958–5963.
- (26) Dock-Bregeon, A.-C., Rees, B., Torres-Larios, A., Bey, G., Caillet, J., and Moras, D. (2004) Achieving Error-Free Translation: The Mechanism of Proofreading of Threonyl-tRNA Synthetase at Atomic Resolution. *Mol. Cell* 16, 375–386.
- (27) Kumar, S., Das, M., Hadad, C. M., and Musier-Forsyth, K. (2013) Aminoacyl-tRNA Substrate and Enzyme Backbone Atoms Contribute to Translational Quality Control by YbaK. *J. Phys. Chem. B* 117, 4521–4527.
- (28) Kumar, S., Das, M., Hadad, C. M., and Musier-Forsyth, K. (2012) Substrate and enzyme functional groups contribute to translational quality control by bacterial prolyl-tRNA synthetase. *J. Phys. Chem. B* 116, 6991–6999.
- (29) Ruan, B., and Soll, D. (2005) The bacterial YbaK protein is a Cys-tRNA^{Pro} and Cys-tRNA^{Cys} deacylase. *J. Biol. Chem.* 280, 25887–25891.
- (30) An, S., and Musier-Forsyth, K. (2005) Cys-tRNA^{Pro} Editing by *Haemophilus influenzae* YbaK via a Novel Synthetase-YbaK-tRNA Ternary Complex. *J. Biol. Chem.* 280, 34465–34472.
- (31) Fukunaga, R., and Yokoyama, S. (2006) Structural Basis for Substrate Recognition by the Editing Domain of Isoleucyl-tRNA Synthetase. *J. Mol. Biol.* 359, 901–912.
- (32) So, B. R., An, S., Kumar, S., Das, M., Turner, D. A., Hadad, C. M., and Musier-Forsyth, K. (2011) Substrate-mediated Fidelity Mechanism Ensures Accurate Decoding of Proline Codons. *J. Biol. Chem.* 286, 31810–31820.
- (33) Fukunaga, R., and Yokoyama, S. (2006) Structural basis for substrate recognition by the editing domain of isoleucyl-tRNA synthetase. *J. Mol. Biol.* 359, 901–912.
- (34) Jakubowski, H. (2013) The Mechanism and Consequences of Homocysteine Incorporation Into Protein in Humans. *Phosphorus, Sulfur Silicon Relat. Elem.* 188, 384–395.
- (35) Jakubowski, H., and Fersht, A. R. (1981) Alternative pathways for editing non-cognate amino acids by aminoacyl-tRNA synthetases. *Nucleic Acids Res.* 9, 3105–3117.
- (36) Jakubowski, H. (1996) The synthetic/editing active site of an aminoacyl-tRNA synthetase: Evidence for binding of thiols in the editing subsite. *Biochemistry* 35, 8252–8259.
- (37) Serre, L., Verdon, G., Choinowski, T., Hervouet, N., Risler, J.-L., and Zelwer, C. (2001) How methionyl-tRNA synthetase creates its amino acid recognition pocket upon L-methionine binding. *J. Mol. Biol.* 306, 863–876.
- (38) Hendrickson, T. L., and Schimmel, P. (2003) Transfer RNA-dependent amino acid discrimination by aminoacyl-tRNA synthetases. *Translation mechanisms*, 34–64.
- (39) Tuite, N. L., Fraser, K. R., and O'Byrne, C. P. (2005) Homocysteine toxicity in *Escherichia coli* is caused by a perturbation of branched-chain amino acid biosynthesis. *J. Bacteriol.* 187, 4362–4371.
- (40) Molecular Operating Environment (MOE) (2015) Chemical Computing Group Inc., Montreal.
- (41) Nakanishi, K., Ogiso, Y., Nakama, T., Fukai, S., and Nureki, O. (2005) Structural basis for anticodon recognition by methionyl-tRNA synthetase. *Nat. Struct. Mol. Biol.* 12, 931–932.
- (42) Nakama, T., Nureki, O., and Yokoyama, S. (2001) Structural basis for the recognition of isoleucyl-adenylate and an antibiotic, mupirocin, by isoleucyl-tRNA synthetase. *J. Biol. Chem.* 276, 47387–47393.
- (43) Kumar, S., Huang, C., Zheng, G., Bohm, E., Bhatele, A., Phillips, J. C., Yu, H., and Kale, L. V. (2008) Scalable molecular dynamics with NAMD on the IBM Blue Gene/L system. *IBM J. Res. Dev.* 52, 177–188.
- (44) Frisch, M. J., Trucks, G. W., Schlegel, H. B., Scuseria, G. E., Robb, M. A., Cheeseman, J. R., Scalmani, G., Barone, V., Mennucci, B., Petersson, G. A., Nakatsuji, H., Caricato, M., Li, X., Hratchian, H. P., Izmaylov, A. F., Bloino, J., Zheng, G., Sonnenberg, J. L., Hada, M., Ehara, M., Toyota, K., Fukuda, R., Hasegawa, J., Ishida, M., Nakajima, T., Honda, Y., Kitao, O., Nakai, H., Vreven, T., Montgomery, J. A., Jr., Peralta, J. E., Ogliaro, F., Bearpark, M., Heyd, J. J., Brothers, E., Kudin, K. N., Staroverov, V. N., Keith, T., Kobayashi, R., Normand, J., Raghavachari, K., Rendell, A., Burant, J. C., Iyengar, S. S., Tomasi, J., Cossi, M., Rega, N., Millam, J. M., Klene, M., Knox, J. E., Cross, J. B., Bakken, V., Adamo, C., Jaramillo, J., Gomperts, R., Stratmann, R. E., Yazyev, O., Austin, A. J., Cammi, R., Pomelli, C., Ochterski, J. W., Martin, R. L., Morokuma, K., Zakrzewski, V. G., Voth, G. A., Salvador, P., Dannenberg, J. J., Dapprich, S., Daniels, A. D., Farkas, O., Foresman, J. B., Ortiz, J. V., Cioslowski, J., and Fox, D. J. (2009) *Gaussian 09*, Gaussian, Inc., Wallingford, CT.
- (45) Bearpark, M. J., Ogliaro, F., Vreven, T., Boggio-Pasqua, M., Frisch, M. J., Larkin, S. M., and Robb, M. A. (2007) CASSCF calculations for excited states of large molecules: Choosing when to use the RASSCF, ONIOM and MMVB approximations. In *Computation in Modern Science and Engineering Volume 2, Parts a and B* (Simos, T. E., and Maroulis, G., Eds.) pp 583–585, American Institute of Physics, Melville, NY.
- (46) Dapprich, S., Komaromi, I., Byun, K. S., Morokuma, K., and Frisch, M. J. (1999) A new ONIOM implementation in Gaussian98. Part I. The calculation of energies, gradients, vibrational frequencies and electric field derivatives. *J. Mol. Struct.: THEOCHEM* 461–462, 1–21.
- (47) Vreven, T., Byun, K. S., Komaromi, I., Dapprich, S., Montgomery, J. A., Morokuma, K., and Frisch, M. J. (2006) Combining quantum mechanics methods with molecular mechanics methods in ONIOM. *J. Chem. Theory Comput.* 2, 815–826.
- (48) Becke, A. D. (1993) A new mixing of Hartree–Fock and local density-functional theories. *J. Chem. Phys.* 98, 1372–1377.
- (49) Case, D. A., Cheatham, T. E., Darden, T., Gohlke, H., Luo, R., Merz, K. M., Onufriev, A., Simmerling, C., Wang, B., and Woods, R. J. (2005) The Amber biomolecular simulation programs. *J. Comput. Chem.* 26, 1668–1688.
- (50) Handy, N. C., and Cohen, A. J. (2001) Left-right correlation energy. *Mol. Phys.* 99, 403–412.
- (51) Crepin, T., Schmitt, E., Mechulam, Y., Sampson, P. B., Vaughan, M. D., Honek, J. F., and Blanquet, S. (2003) Use of analogues of methionine and methionyl adenylate to sample conformational changes during catalysis in *Escherichia coli* methionyl-tRNA synthetase. *J. Mol. Biol.* 332, 59–72.
- (52) Banik, S. D., and Nandi, N. (2012) Mechanism of the activation step of the aminoacylation reaction: a significant difference between class I and class II synthetases. *J. Biomol. Struct. Dyn.* 30, 701–715.
- (53) Using PropKa [Bas, D. C., Rogers, D. M., and Jensen, J. H. (2008) Very fast prediction and rationalization of pK_a values for protein-ligand complexes. *Proteins: Struct., Funct., Genet.* 73, 765–783], Asp259 is predicted to have a pK_a value of 7.5 while the other Asp residues in MetRS generally have pK_a's in the range of 2.5–6.3.
- (54) Jakubowski, H. (1997) Aminoacyl thioester chemistry of class II aminoacyl-tRNA synthetases. *Biochemistry* 36, 11077–11085.